



HAL
open science

Design and Methodology of Silicon Carbide High Voltage Termination Extension for Small Area BJTs

Ali Ammar, Luong Viêt Phung, Dominique Planson, Hervé Morel, Camille Sonneville

► **To cite this version:**

Ali Ammar, Luong Viêt Phung, Dominique Planson, Hervé Morel, Camille Sonneville. Design and Methodology of Silicon Carbide High Voltage Termination Extension for Small Area BJTs. Materials Science Forum, 2022, 1062, pp.613-618. 10.4028/p-vms03o . hal-03703994

HAL Id: hal-03703994

<https://hal.science/hal-03703994>

Submitted on 24 Jun 2022

HAL is a multi-disciplinary open access archive for the deposit and dissemination of scientific research documents, whether they are published or not. The documents may come from teaching and research institutions in France or abroad, or from public or private research centers.

L'archive ouverte pluridisciplinaire **HAL**, est destinée au dépôt et à la diffusion de documents scientifiques de niveau recherche, publiés ou non, émanant des établissements d'enseignement et de recherche français ou étrangers, des laboratoires publics ou privés.

Design and Methodology of Silicon Carbide High Voltage Termination Extension for Small Area BJTs

Ali Ammar^{1,a*}, Luong Viet Phung^{1,b}, Dominique Planson^{1,c}, Herve Morel^{1,d}
Camille Sonnevile^{1,e}

¹Univ Lyon, INSA Lyon, Université Claude Bernard Lyon 1, Ecole Centrale de Lyon, CNRS, AMPERE, F-69621, Lyon, France

^aali.ammar@insa-lyon.fr, ^bluong-viet.phung@insa-lyon.fr, ^cdominique.planson@insa-lyon.fr,
^dherve.morel@insa-lyon.fr, ^ecamille.sonneville@insa-lyon.fr

Keywords: Bipolar Power Devices, Silicon Carbide, Junction Termination Extension, High Electric Field, TCAD Modeling

Abstract: An optimized termination extension tutorial is reported for a small area ($\approx 1\text{mm}^2$) 4H-SiC NPN BJT. The extension system is based on a parametric JTE with isolation rings. Additional aspects such as (1) MESA angle, (2) relieving electric field on the base-drift junction, and (3) blocking the electric field from reaching border structure are investigated. A breakdown voltage greater than 10 kV is recorded, when drift region is n-doped to $8 \times 10^{14} \text{ cm}^{-3}$.

Introduction

4H-SiC power bipolar devices are considered one of the most reasonable candidates for low-loss and high power semiconductor devices when compared to Silicon (Si) due to (1) a high bandgap allowing it to reach a low intrinsic carrier density even when operating over high temperatures (greater than 500 °C) [1], (2) a high saturation drift velocity enabling the operation over high frequencies, and (3) a huge breakdown electric field resulting in the reduction of ON resistance (R_{ON}) plus avoiding a second breakdown avalanche effect [2]. Similarly, 4H-SiC power BJTs, are free from gate oxide problems giving it the ability to sustain high currents with low-voltage drop when compared to SiC MOSFETs [3]. Since BJTs are current controlled devices, making it a disadvantage over MOSFETs, an input drive current is needed on the base terminal in the on-state operation mode leading to an increase in the total power dissipation of the device, thus it is always useful to maximize the current gain in BJTs. The recent reported high voltage 4H-SiC BJTs include a 10 kV open-base breakdown voltage (BV_{CEO}) and specific on-resistance of $130 \text{ m}\Omega \cdot \text{cm}^2$ at (RT) with a $120 \mu\text{m}$, $6 \times 10^{14} \text{ cm}^{-3}$ n-doped drift layer [4]; a 15 kV BV_{CEO} at a leakage current of 0.1 mA/cm^2 with $125 \mu\text{m}$ drift layer n-doped to $1.1 \times 10^{14} \text{ cm}^{-3}$ [5], and a 9.2 kV BV_{CEO} with a $50 \mu\text{m}$, $7 \times 10^{14} \text{ cm}^{-3}$ n-doped drift layer and $R_{SP_ON} = 78 \text{ m}\Omega \cdot \text{cm}^2$ [6]. For high electric field bipolar applications, it is mandatory to implant a highly sophisticated base-drift junction termination extension (JTE) system, which serves in minimizing the electric field plate crowd generated at the MESA edge of the power device. Several approaches were applied to optimize the extension performance; (1) by applying variations over the length and etching depth of the JTE [7], (2) by implanting different doses over the total length of the JTE [8], and (3) by the addition of extra implanted rings [9]. This paper presents different design methodologies for high-voltage SiC BJT termination for obtaining both high-open-emitter (BV_{CBO}) and high open-base (BV_{CEO}) breakdown voltage greater than 10 kV based on simulation measurements done using Synopses TCAD [10]. The realized results are relative to several technical models associated to the SiC simulation parameters given by TCAD, which were used as follows: *Arora* model for Doping Dependence., *Caughey-Thomas* model for High Field Dependence, *Scharfetter* and *VanOverstraetendeMan* used for Recombination and Impact Ionization models, and finally *Bandgap Narrowing* for the band gap model.

SiC BJT Termination Model and Technology

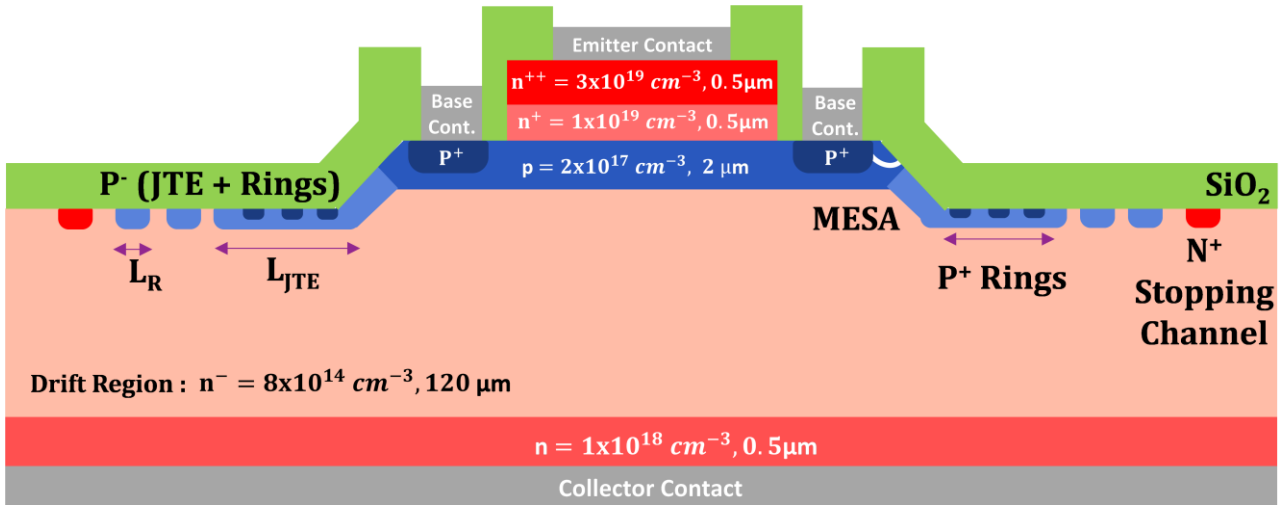


Figure 1: Schematic cross-sectional view of a BJT structure with optimized termination

Figure 1 represents an illustration of a 4H-SiC NPN optimized BJT structure. The structure is built with a 0.5 μm, $1 \times 10^{18} \text{ cm}^{-3}$ n-doped collector layer. The lowly n-doped drift layer has a thickness of 120 μm and a doping concentration $8 \times 10^{14} \text{ cm}^{-3}$. The 2 μm base layer is p-doped to $2 \times 10^{17} \text{ cm}^{-3}$, with 400 nm highly p⁺ implants under the base contacts to ensure a low resistive ohmic contact. The 0.5 μm emitter layer is n-doped to $1 \times 10^{19} \text{ cm}^{-3}$ meeting another 0.5 μm highly n-doped emitter contact layer. Theoretically, the highest breakdown voltage of a PN junction with such drift parameters can reach to 14 kV according to Equation 1, where BV represents the blocking voltage in volts, EF_{\max} is maximum electrical field that SiC can sustain in V/cm, ϵ_s is the dielectric permittivity of the semiconductor material, and N_D is the doping concentration of the drift region in cm^{-3} .

$$BV = \frac{EF_{\max}^2 \epsilon_s}{2eN_D} \dots \dots \dots \text{(Equation 1, [11])}$$

The thickness of the epitaxial layer also influences the breakdown voltage, since the electrical field E_B can be expressed as follows:

$$EF_{\max}^2 = q \frac{N_D W_D}{\epsilon_s} \dots \dots \dots \text{(Equation 2, [11])}$$

where W_D is the drift thickness in meters, giving another form of the blocking voltage:

$$BV = q \frac{N_D W_D^2}{2\epsilon_s} \dots \dots \dots \text{(Equation 3, [11])}$$

From Equations 1 and 3, we realize that increasing W_D , and decreasing N_D , both serve in increasing the blocking voltage. This feature can be observed in [8], where the highest breakdown voltage for a BJT to-date is recorded 21 kV. This lab in Kyoto University/Japan, in addition to an optimized termination extension and a proper fabrication process, was able to reach this value with a very low $N_D = 2.3 \times 10^{14} \text{ cm}^{-3}$ and a W_D greater than 180 μm. Putting these values in Equation 1, a maximum theoretical breakdown voltage up to 50 kV can be obtained, which is considered far from the recorded results. Normally, it is impossible to reach the theoretical breakdown due to electric field crowding close to junction edges, but research is always working to get near this value by optimizing the termination extension. Figure 1 describes several approaches when designing an optimized extension.

From geometrical point of view, fabrication of MESA structures with negative inclination aid in avoiding problems such as edge breakdown due to a significant reduction of electric field when compared to the bulk one [12].

Figure 2, shows the electric field behavior of same BJT structure but with different MESA angles. An increase in the angle reduces the electric field crowding generated on the junction. Relieving this electrical field crowding effect is also done by implanting P⁺ isolation rings. These rings can be capped along the JTE as in Figure 1 and integrated at the edge of structure with an ohmic contact performing a PN isolation diode as described in [13].

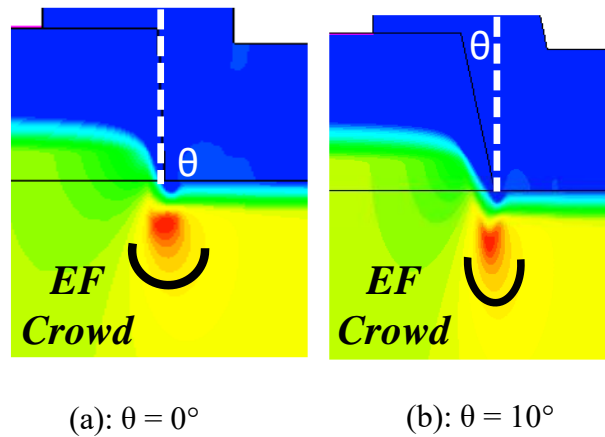


Figure 2: Electrical field (EF) distribution at MESA with various angle θ : (a) $\theta = 0^\circ$, (b) $\theta = 10^\circ$

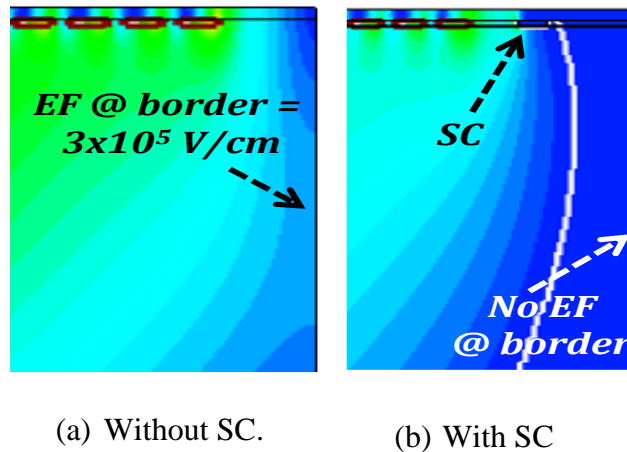


Figure 3: Electrical field (EF) behavior at device border: (a) without stopping channel, (b) with SC.

The efficiency of the JTE is influenced by parameters such as the length (L_{JTE}), and the implanted dose (D_{JTE}). The idea is to provide a smooth flow for the electric field by choosing the suitable dose given for the implanted JTE along its length. The chosen dose should be relative to the base doping concentration, for permitting a continuous flow all over the structure. The thickness of the JTE is limited and fixed to $1\mu\text{m}$, as we vary the dose.

Moreover, is it possible to complete the extension by adjoining rings with the same dose and thickness associated to the JTE (Figure 1). The performance of the rings is relative to their number (N_{Rings}) and the space given between them (S_{Rings}), which may vary between each ring. The rings length (L_R) which is not considered a critical parameter is fixed to $5\mu\text{m}$. The number of rings with their associated spaces plus the L_{JTE} determines the overall length of the termination system. This length is important when dealing with small sized structures.

In normal cases, no electric field crowd should be present at the edge of the structure, and hence an isolation length should be given after the given extension system. For small structures, where no to little space is available, a highly n+-doped stop channel can be added after the termination extension (Figure 1) in order to prevent the lateral electric field from reaching the chip edge which is a phenomenon where capability of breakdown voltage decreases as shown in Figure 3.

Results and Discussion

Table 1 describes three different general small BJT structures with different designs. Structure 1 as mentioned before refers to an unoptimized device and will be used as a reference. The BV recorded is nowhere from reaching the 10 kV, with a 0% of enhancement due to the absence of JTE and Rings. Structure 2 is built just with a JTE. Several lengths between 250 μm and 500 μm were tested with different doses in order to detect the optimum length and dose that match the base doping we have. No rings are integrated in this structure and the recorded BV is increased by 300% since the breakdown voltage obtained is almost triple the one we got from structure 1, translating the ability of peripheral protection to get closer to the theoretical 1D target. After dealing with the JTE parameters, an isolation ring system is added to structure 3 with constant spacing between them. This structure burdened more the electrical field and hence increased significantly the efficiency of the system to reach up to 430%. Finally, referring to the electrical field profile shown in Figure 4 we can clearly notice the importance and potential of adding a JTE and ring system on the electric field. The continuous curve in Figure 4 refers to the electric field associated to structure 1. We realize the peak of the curve is located immediately at the base-drift junction, and then the field sharply vanishes, which explains the low breakdown voltage with such a structure. Paradoxically, the dashed curve represents an optimized structure. We notice how the electric field is distributed all over the structure. The first two peaks of this field determine the starting and ending point of the JTE, while the following ones represent the electric field on each ring border to reach the last one. It is highly recommended to conserve or keep the same electric field along the border of the JTE and rings, in other words; keeping the same level for each peak. This phenomenon also affects the ability of increasing the breakdown voltage and it is controlled by the number and space given between each ring.

Table 1: Variation of breakdown voltage as function of structure design

Structure	JTE	L_{JTE} [μm] D_{JTE} [$\times 10^{13} \text{ cm}^{-2}$]	N_{Rings}	BV_{CBO} [kV]
1	Absence ✗	Absence ✗ Absence ✗	Absence ✗ Absence ✗	3
2	Presence ✓	$L_{\text{JTE}} \in [250, 500]$ $D_{\text{JTE}} \in [0.8, 1.5]$	Absence ✗ Absence ✗	9
3	Presence ✓	$L_{\text{JTE}} \in [250, 500]$ $D_{\text{JTE}} \in [0.8, 1.5]$	$N_{\text{Rings}} \in [1, 8]$	12.6

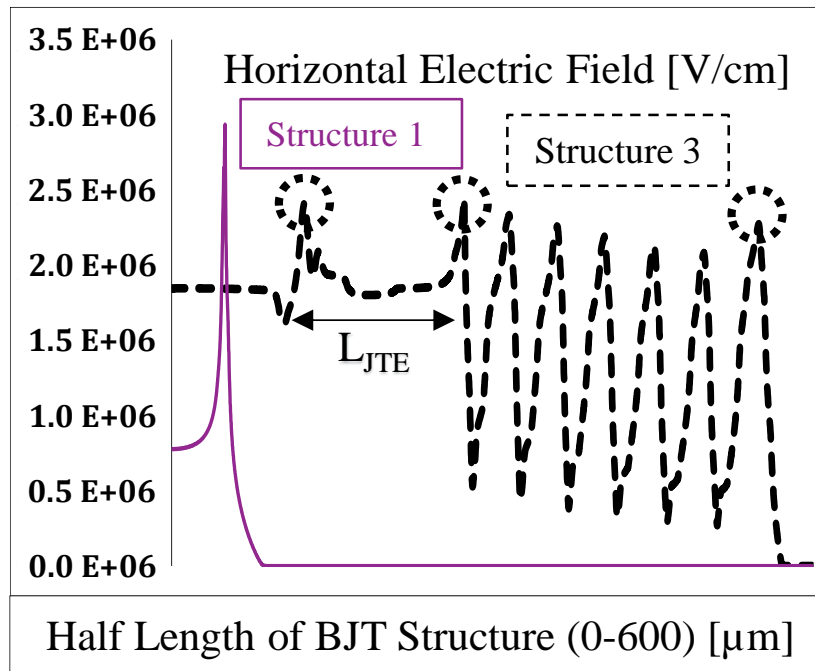


Figure 4: Variation of electrical field as a function of JTE and Rings presence

Conclusion

A high power, with small area 4H-SiC NPN bipolar transistor structure with optimized termination extension was investigated in this paper. The termination is highly effective and efficient. A targeted breakdown voltage was reached with a proper electric profile all over the structure. A final structure was ended up with specific parameters where the breakdown voltage recorded is 12.6 kV which forms 90% from the theoretical value (14 kV) with 120 μm drift thickness n-doped to $8 \times 10^{14} \text{ cm}^{-3}$. Additional points were discussed concerning high P^+ doped implanted rings to decrease the electric field peak at the base-drift junction, and highly N^+ doped stopping channel for the aim of blocking high electric field on the edge of the structure.

Acknowledgement

This work was supported by a grant overseen by the French National Research Agency (ANR), the project HV-PhotoSW, ANR-18-CE05-0020-01.

References

- [1] M. Locatelli, «Silicon carbide against silicon: a comparison in terms of physical properties, technology and electrical performance of power devices,» *Journal de Physique III, EDP Sciences*, vol. 1, pp. 1101 - 1110, 1993.
- [2] J. A. Cooper et A. Agarwal, «SiC Power-Switching Devices—The Second Electronics Revolution» *PROCEEDINGS OF THE IEEE*, vol. 90, pp. 956-968, 2002.
- [3] S. Krishnaswami, A. Agarwal, S. H. Ryu, C. Capell, J. Richmond, J. Palmour, S. Balachandran, P. T. Chow, S. Bayne, B. Geil, K. Jones et C. Scozzie, «1000-V, 30-A 4H-SiC BJTs With High Current Gain,» *IEEE ELECTRON DEVICE LETTERS*, vol. 26, pp. 2474-2481, 2005.

- [4] Q. J. Zhang et R. Callanan, «10 kV, 10 A Bipolar Junction Transistors and Darlington Transistors on 4H-SiC,» *Materials Science Forum*, vol. 1 , pp. 1025-1028, 2010.
- [5] A. Salemi et K. Jacobss, «15 kV-Class Implantation-Free 4H-SiC BJTs 15 kV-Class Implantation-Free 4H-SiC BJTs,» *IEEE ELECTRON DEVICE LETTERS*, vol. 39, pp. 63-66, 2018.
- [6] J. Zhang, J. H. Zhao, P. Alexandrov et T. Burke, «Demonstration of first 9.2 kV 4H-SiC bipolar junction transistor,» *ELECTRONICS LETTERS*, vol. 40, 2004.
- [7] A. Salemi, «Area- and Efficiency-Optimized Junction Termination for a 5.6 kV SiC BJT Process with Low ON-Resistance,» *International Symposium on Power Semiconductor Devices*, 2015.
- [8] H. Miyake, «21-kV SiC BJTs With Space-Modulated Junction Termination Extension,» *IEEE ELECTRON DEVICE LETTERS*, vol. 33, 2012.
- [9] D. PLANSON et L. V. PHUNG, «Edge termination design improvements for 10 kV 4H-SiC bipolar diodes,», vol. 1, pp. 609-612, 2013.
- [10] Sentaurus, *TCAD Simulation Tool by Synopses Inc., ver. Q (2019)*.
- [11] B. Buono, «Simulation and Characterization of Silicon Carbide Power Bipolar Junction Transistors,» KTH Royal Institute, Stockholm, 2012.
- [12] N. M. Lebedeva, N. D. Il'inskaya et P. A. Ivanov, «Edge-Termination Technique for High-Voltage Mesa-Structure 4H-SiC Devices: Negative Beveling,» *PHYSICS OF SEMICONDUCTOR DEVICES*, vol. 54, pp. 258-262, 2020.
- [13] S. Liang, J. Wang et F. Fang, «Optimization Design of Isolation Rings in Monolithically Integrated 1200V SiC Transistor and Anti-Parallel Diode for Improved Blocking Voltage,» *IEEE Journal of Emerging and Selected Topics in Power Electronics*, vol. 7, pp. 1513-1518, 2019.